Carpathian Journal of Earth and Environmental Sciences, August 2018, Vol. 13, No. 2, p. 465 - 476; DOI:10.26471/cjees/2018/013/040

# GEOSPATIAL TECHNIQUES FOR THE ANALYSIS OF HYPSOMETRIC PARAMETERS OF A HUMID TROPICAL RIVER BASIN, SOUTH WESTERN GHATS, INDIA

**Balakrishnan Nair AJAYKUMAR[1*] & Girish GOPINATH[2]**

*[1]Department of Mining and Geology, Government of Kerala, India*
*[2]Geomatics Division, Centre for Water Resources Development and Management, Kozhikode, Kerala, India*
*[*]Corresponding author, e-mail: jemnair@gmail.com*

**Abstract:** Hypsometric analysis is a significant tool for assessing the influence of geologic and tectonic factors on topography and also to prioritize sub-watersheds based on soil erosion and runoff. To understand the type of erosive processes and relative age of land forms, hypsometric analysis is carried out for all the 15 sub-basins of Meenachil River Basin, a humid tropical river basin of the Western Ghats, Kerala. Hypsometric analysis was performed on SRTM DEM (90m resolution) to derive the hypsometric parameters and the curves for each sub- watershed as well as to entire basin using CalHypso an Add-on tool to Arc GIS 9.2 and the statistical data like hypsometric integral, skewness and kurtosis were also determined. Based on the shape of hypsometric curves and value of hypsometric parameters, the geomorphic stages of the sub watersheds were identified, and the erosion status of the watersheds was finally predicted based on the geomorphic stages. Among the 15 sub-watersheds, six sub-watersheds indicate the in-equilibrium stage as the Hypsometric Integral > 0.3. The analysis also revealed that the lithologic and structural differences between areas or recent minor uplifts for sub-watersheds SW4, SW5, SW8, SW11, SW12 and SW13. The pattern of the hypsometric curves of SW6, SW7, SW14 and SW15 suggested that the formation of alluvial deposits made the watershed favourable for groundwater re-charge.

**Key words:** Meenachil River Basin, Digital Elevation Model, CalHypso, Hypsometric Curve, Hypsometric Integral.

## 1. INTRODUCTION

The hydrological response of watersheds to precipitation events depends on the mechanisms of runoff generation, in particular on the partitioning between surface and subsurface discharge to the channel network, where the topography plays a significant role in determining the basin response (Schumm 1956; Howard 1990; Tarboton et al., 1992; Marani et al., 2001; Ivanov et al., 2004a; Bertoldi et al., 2006; Ascione et al., 2008). A strong interplay exists between basin geomorphic shape and its hydrological response, which ultimately defines the impact of the outcome of erosional processes on landscape form (Rodri′guez-Iturbe & Valdes 1979; Ijja´sz-Va´squez et al., 1992; Duffy 1996; Tucker & Bras 1998; Ivanov et al., 2004b). While the hydrological processes depend on many basin properties, the relief ratio and catchment volume design important roles in determining runoff (Zecharias & Brutsaert 1988; Hutchinson 1989; Eltahir & Yeh 1999; Luo & Harlin 2003). Hypsometric analysis helps to assess the influence of geologic and tectonic factors on topography. According to Harlin 1978, the hypsometric curve is treated as a cumulative probability distribution function; the form of the curve can be quantitatively described by a series of statistical moments, such as skewness and kurtosis of its density function. Further these parameters or attributes are sensitive to subtle changes in overall basin slope and basin development as the mass is removed by erosion over a long geological time period (Harlin 1980). The statistical characteristics of hypsometric analysis include hypsometric integral (Ea), hypsometric curve, co-ordinates of slope inflection points,

hypsometric skewness and kurtosis etc.

The relief ratio and catchment volume can be concisely captured through the hypsometric (area-altitude) curve and the hypsometric curve is typically represented as the distribution of the relative height (h/H) with relative area (a/A) (Langbein 1947; Strahler 1952; Pike & Wilson 1971). Despite that the hypsometric curve aggregates the three-dimensional basin structure, its shape has been related to the hydrograph peak and travel time (Harlin 1984; Luo 1998; Oertel 2001; Luo & Harlin 2003; Latron & Gallart 2007; Liyanagamage & Hewa 2012; Kedareswarudu et al., 2013) and the regional groundwater base flow (Marani et al., 2001; Vivoni et al., 2007). Hypsometric analysis is not only a significant tool for identifying the geological stages of development but also for prioritization of sub-watersheds based on soil erosion and runoff. Many works have been reported on Hypsometric analysis using GIS and D'Alessandro et al., (1999) emphasises the significance of Hypsometric analysis in the study of morphoevolution of drainage basin by portraying the evolution of the land tectonic history using hypsometry.

The hypsometric curve has been widely used to interpret stages of landscape evolution due to uplift and denudation (Ijja´sz-Va´squez et al., 1992; Ohmori 1993; Tucker & Bras 1998; Willgoose & Hancock 1998; Brocklehurst & Whipple 2004; Cheng et al., 2012). Previous studies also showed that basin hypsometry is related to the size, shape, and relief of the basin (Strahler 1952; Weissel et al., 1994; Vivoni et al., 2004; 2005; Vivoni et al., 2008, Markose & Jayappa, 2011) as well as other factors such as the dominant erosion process (Moglen & Bras 1995; Willgoose & Hancock 1998; Luo 2000; Hancock & Willgoose 2001; Azor et al., 2002; Chen et al., 2003; Korup, 2006; Singh 2009; Ramu & Mahalingam 2012), sensitiveness to both uplift rates and the erosional resistance of lithological units (Lifton & Chase 1992; Hurtrez et al., 1999; Chen et al., 2003; Walcott & Summerfield 2008; Sivakumar et al., 2011) and rapid tectonic activities (Keller & Pinter 1996; Hurtrez et al., 1999; Chen et al., 2003; Korup et al., 2005; 2007; Pedrera et al., 2009; Barbero et al., 2010; Shahzad & Gloaguen 2011; Mahmood et al., 2012). Practical applications of hypsometric analysis are foreseen in hydrology, soil erosion and sedimentation studies and military science.

## 2. MATERIALS AND METHODOLOGY

The present study covers 831.661km$^2$ out of the total 1272 km$^2$ area of the Meenachil River Basin and is located between 9°32' and 9°51'N latitudes and 76°29' and 76°56' E longitudes (Fig. 1). Meenachil River, one of the major rivers of Kerala, originates from Kolahalamedu at an elevation of 1156m above MSL. The major river draining has a length of 78km. The river basin enjoys the humid tropical climate with an average rainfall of 3120mm/year of which 1646mm is received during the Southwest monsoon. The river has a total annual yield of 2349 million cubic meters and annual utilizable yield of 1110 million cubic meters. As far as the ground water resource is concerned, the area falls in the category of 'white', which means that only less than 65% of the ground water is utilised. The Meenachil watershed is divided into 15sub-watersheds, 47 mini-watersheds and 114 micro-watersheds.

The Hypsometric analysis of the Meenachil River Basin was based on published Survey of India topographical maps on a 1:50,000 scale. The hard copy topographic map was scanned and geo-referenced in ERDAS IMAGINE 9.1 and onscreen digitization process was carried out using Arc GIS 9.2 for preparing the stream network. The designation of the stream order is based on the hierarchy ranking of streams proposed by Strahler (1964). The entire River Basin is divided into 15 sub-watersheds which were also digitized from the geo-referenced topographic maps. The SRTM obtained elevation data on a near global scale is used for the present study, for the SRTM data the website http://srtm.csi.cgiar.org was accessed, from which digital elevation model (DEM) of whole basin and 15 sub watersheds were extracted (Fig. 2). Hypsometric curves of each sub watershed and full basin are obtained using CalHypso an Add on tool to Arc GIS 9.2. Statistical data like hypsometric integral, skewness and kurtosis are determined. From the hypsometric curves, maximum concavity, co-ordinates of slope inflection point (I) given by $a^*$ and $h^*$ are calculated using the hypothetical curve (Fig. 3) of Sinha (2002). Based on the shape of hypsometric curves and value of hypsometric parameters, the geomorphic stages of the sub watersheds were identified. Finally based on the geomorphic stage, the erosion status of the sub watersheds is predicted.

## 3. RESULTS AND DISCUSSION

Hypsometry is the graphical representation of the area/elevation function of a drainage basin or the integral of a basin's surface area with respect to its elevation (Langbein 1947; Strahler 1952) (Fig. 4). It is commonly used to assess the extent of basin erosion/relative geomorphic age/degree of excavation and, by extension, the interplay of denudation and tectonic uplift.

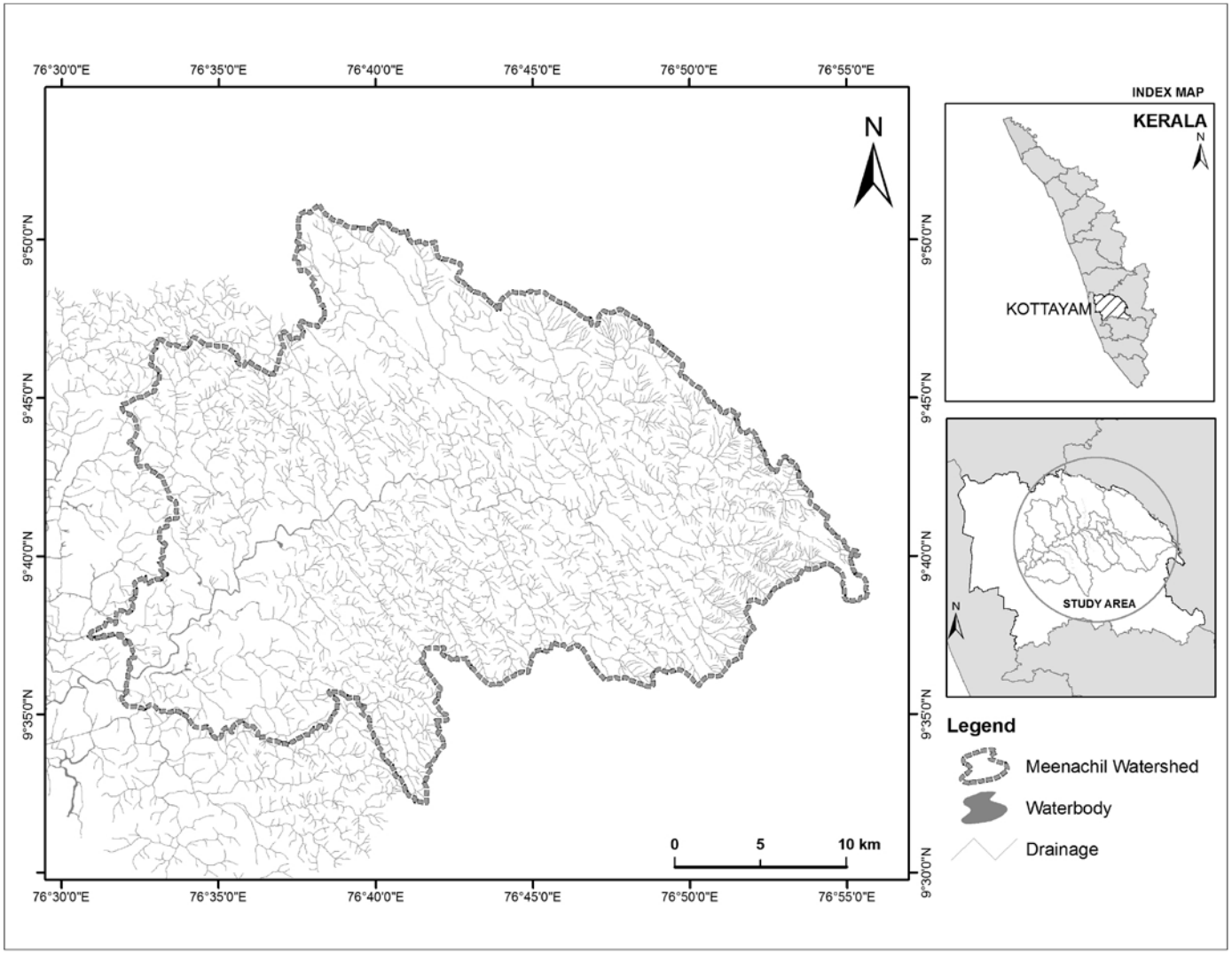


Figure 1. Meenachil River Basin

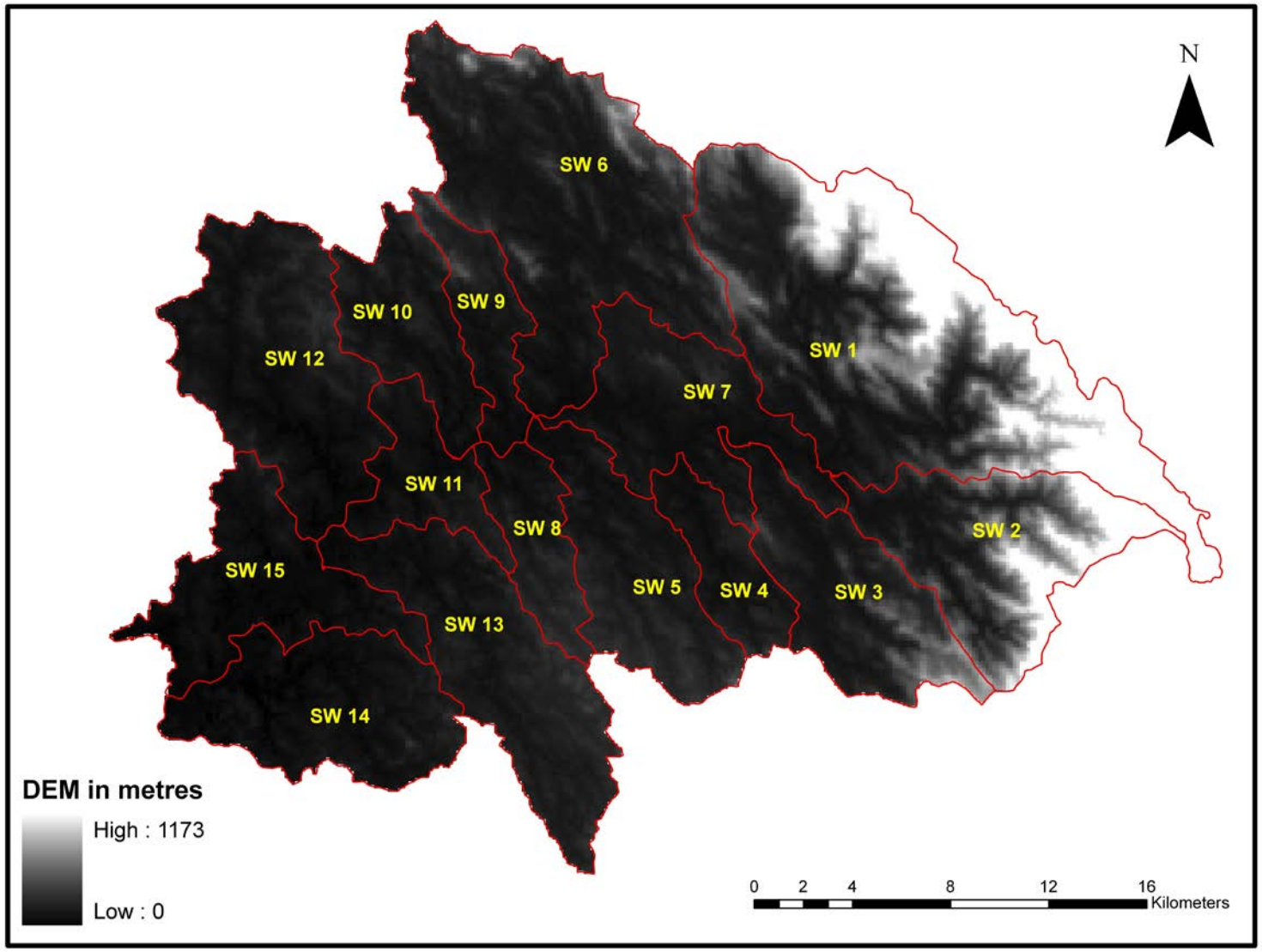


Figure 2. Digital Elevation Model of Meenachil River Basin

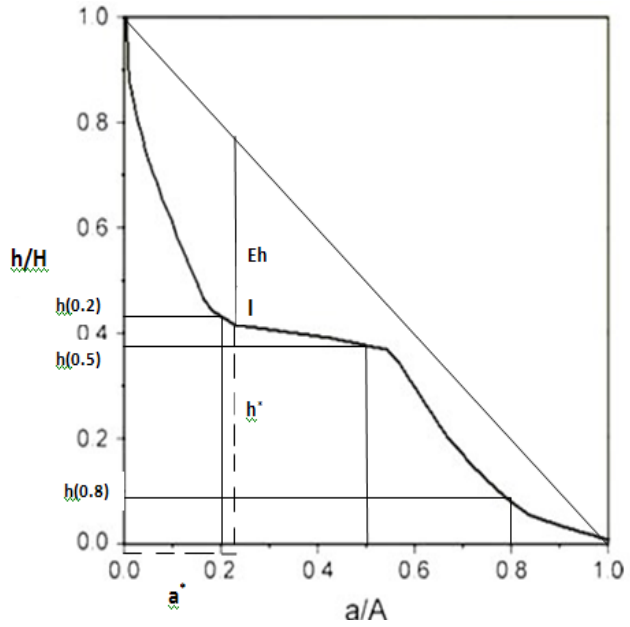


Figure 3. A hypothetical curve defining the hypsometric parameters

A hypsometric integral (a value) and a hypsometric curve (an S-shaped line graph) are outputs of hypsometric analysis (Anderson & Anderson 2010). A hypsometric integral (HI), sometimes called the "elevation/relief ratio", can be calculated for every basin. This index summarizes the basin based on its relief and mean elevation. It provides a general index of erosion or tectonism. HI is useful when comparing several basins to one another. HI values are reported to two decimals. HI values of $\leq$0.30 are considered stable and "mature" in the Davisian sense, while values $\geq$0.60 indicate unstable, "young" basins. Similar HI values may be calculated for basins with very different geomorphic histories. In hypsometric curves, cumulative area and normalized relief are typically plotted on the x-axis and y-axis, respectively. X-axis is scaled from 0-100% (cumulative number of pixels in equal-interval elevation bins of a chosen size). From the hypsometric curves, maximum concavity and co-ordinates of slope inflection point were calculated using the hypothetical curve of Sinha (2002). Y-axis is scaled from 0-1, based on catchment relief (0 value is lowest elevation in basin and 1 is the highest).

In tectonically active areas (uplifting), high HI values (HI >0.50) and convex curves reflect the "young" stage of landscape development (more mass at higher elevations). Balanced S-shaped hypsometric curves (HI ~0.50) indicate relatively young, but still developing basin landscapes. Concave-upward curves (HI < 0.50) usually suggest "older", more extensively excavated basins in tectonically stable landscapes. Similar hypsometric curves can be produced by the interaction of climatic, tectonic, rock type forces, sometimes "overprinting" one another (Bishop et al., 2002).

The percentage hypsometric curve (area-altitude curve) relates horizontal cross-sectional area of a drainage basin to relative elevation above basin mouth. By use of dimensionless parameters, curves can be described and compared irrespective of true scale. Curves show distinctive differences both in sinuosity of form and in proportionate area below the curve, here termed the hypsometric integral. A simple three-variable function provides a satisfactory series of model curves to which most natural hypsometric curves can be fitted. The hypsometric curve can be equated to a mean ground-slope curve if length of contour belt is taken into account (Strahler 1952). The morphology of a river basin plays a fundamental role in the dynamics of surface and subsurface runoff generation. Substantial modifications of the basin morphologic system can lead to changes in the river basin response to precipitation events. The hypsometric curve is a concise, but powerful instrument that encloses the necessary features to represent the form of a watershed and its evolution. It is also able to describe the hydrologic behaviour of a river basin through a set of parameters related to the shape of the curve (Di Benedetto et al., 2006).

Hypsometric curves (Fig. 4) are classified into two groups based on the shape. First group includes the curves with upward concavity representing less fluvial processes. The second group is characterized by convex concave shape with, pointing to fluvial and slope wash processes of landforms. Hypsometric curves for all sub-watershed shows upward concave curves but SW4, SW5, SW6, SW7, SW8, SW10, SW11, SW12, SW13, SW14 and SW15 showed downward concave at lower reaches. The convex shape of the graph in the downstream of the sub-watersheds indicates mass accumulation at the mouth. From the hypsometric curves, hypsometric parameters such as hypsometric integral (HI), point of maximum concavity (Eh), coordinates of point of inflection (h*, a*) and height of hypsometric curve at different points have been determined and tabulated in Table 1. Hypsometric integral controls the shape of the hypsometric curve and thereby provides clues for landform evolution (Sinha 2002). Downward concave hypsometric curves show high hypsometric integral. Based on the value of hypsometric integral, the sub watersheds are classified into 3 groups and they are

(1) Old (0 < HI < 0.3),
(2). Mature (0.3 < HI < 0.6) and
(3). Young (0.6 <HI < 1).

**Table - 1: Hypsometric parameters of Meenachil River Basin and its 15 sub-watersheds**

| Watershed | Area ($km^2$) | Hypsometric Integral (Ea) | Maximum concavity (Eh) | a* | h* | h (0.2) | h (0.5) | h (0.8) |
|---|---|---|---|---|---|---|---|---|
| SW1 | 156.347 | 0.2701 | 4.7 | 0.55 | 0.17 | 0.50 | 0.20 | 0.08 |
| SW2 | 61.071 | 0.2413 | 6.5 | 0.23 | 0.39 | 0.43 | 0.19 | 0.07 |
| SW3 | 47.938 | 0.2390 | 6.8 | 0.30 | 0.28 | 0.38 | 0.19 | 0.12 |
| SW4 | 21.176 | 0.3235 | 5.0 | 0.24 | 0.44 | 0.47 | 0.30 | 0.18 |
| SW5 | 45.978 | 0.3865 | 4.2 | 0.09 | 0.70 | 0.58 | 0.39 | 0.21 |
| SW6 | 110.767 | 0.1935 | 8.5 | 0.14 | 0.30 | 0.26 | 0.17 | 0.13 |
| SW7 | 48.599 | 0.2625 | 6.7 | 0.19 | 0.40 | 0.38 | 0.26 | 0.14 |
| SW8 | 21.883 | 0.4286 | 2.9 | 0.74 | 0.10 | 0.67 | 0.40 | 0.20 |
| SW9 | 22.202 | 0.2535 | 6.4 | 0.13 | 0.45 | 0.39 | 0.24 | 0.12 |
| SW10 | 32.582 | 0.2999 | 6.1 | 0.10 | 0.17 | 0.45 | 0.29 | 0.17 |
| SW11 | 23.808 | 0.3329 | 5.2 | 0.23 | 0.47 | 0.50 | 0.32 | 0.18 |
| SW12 | 71.993 | 0.3173 | 5.1 | 0.14 | 0.53 | 0.49 | 0.30 | 0.19 |
| SW13 | 64.453 | 0.3796 | 4.5 | 0.12 | 0.59 | 0.53 | 0.40 | 0.23 |
| SW14 | 55.065 | 0.2484 | 6.4 | 0.10 | 0.48 | 0.39 | 0.24 | 0.14 |
| SW15 | 47.799 | 0.2092 | 7.1 | 0.34 | 0.15 | 0.30 | 0.18 | 0.11 |
| Meenachil river basin | 831.661 | 0.0834 | 10.1 | 0.15 | 0.14 | 0.10 | 0.05 | 0.04 |

**Table - 2: Statistical moments derived from the hypsometric curves**

| Watershed | Area ($km^2$) | Hypsometric Integral (Ea) | Skewness | Kurtosis | Density Skewness | Density Kurtosis |
|---|---|---|---|---|---|---|
| SW1 | 156.347 | 0.2701 | 0.9852 | 3.1890 | 1.0338 | 3.0855 |
| SW2 | 61.071 | 0.2413 | 0.9195 | 2.7860 | 1.1147 | 2.8912 |
| SW3 | 47.938 | 0.2390 | 0.9461 | 2.8063 | 1.3941 | 3.7327 |
| SW4 | 21.176 | 0.3235 | 0.5575 | 2.1884 | 0.5738 | 1.7878 |
| SW5 | 45.978 | 0.3865 | 0.5259 | 2.2299 | 0.2435 | 1.6032 |
| SW6 | 110.767 | 0.1935 | 0.2823 | 1.5215 | 1.2953 | 2.5998 |
| SW7 | 48.599 | 0.2625 | 0.5428 | 2.0204 | 0.8752 | 2.0515 |
| SW8 | 21.883 | 0.4286 | 0.5623 | 2.3379 | 0.1464 | 1.6817 |
| SW9 | 22.202 | 0.2535 | 0.6233 | 2.1496 | 0.8606 | 2.0793 |
| SW10 | 32.582 | 0.2999 | 0.5130 | 2.1008 | 0.5708 | 1.7124 |
| SW11 | 23.808 | 0.3329 | 0.5699 | 2.1995 | 0.5865 | 1.7904 |
| SW12 | 71.993 | 0.3173 | 0.5786 | 2.1933 | 0.6225 | 1.8102 |
| SW13 | 64.453 | 0.3796 | 0.4384 | 2.0523 | 0.2710 | 1.4345 |
| SW14 | 55.065 | 0.2484 | 0.5764 | 2.0706 | 0.8420 | 2.0085 |
| SW15 | 47.799 | 0.2092 | 0.4961 | 1.8407 | 1.0721 | 2.2990 |
| Meenachil river basin | 831.661 | 0.0834 | -0.2837 | 0.9570 | 1.6064 | 3.0615 |

**Table - 3: Inference on Hypsometric parameters**

| Watershed | Area ($km^2$) | Hypsometric Integral (Ea) | Basin response to | | | | |
|---|---|---|---|---|---|---|---|
| | | | *GSD | Hydrology | Erosion | Tectonism | Lithology |
| SW1 | 156.347 | 0.2701 | Old | Intensified run-off | Prone to erosion | Less influenced | Homogenous |
| SW2 | 61.071 | 0.2413 | Old | Intensified run-off | Prone to erosion | Less influenced | Homogenous |
| SW3 | 47.938 | 0.2390 | Old | Intensified run-off | Prone to erosion | Less influenced | Homogenous |
| SW4 | 21.176 | 0.3235 | Mature | Uniform water discharge | Less eroded surface | Partially influenced | Intrusions and exposed to denudation |
| SW5 | 45.978 | 0.3865 | Culminating stage | Uniform water discharge | Less eroded surface | Influenced | Intrusions and exposed to denudation |
| SW6 | 110.767 | 0.1935 | Very Old | Ground water potential | Deposition at lower reaches | Less influenced | Homogenous |
| SW7 | 48.599 | 0.2625 | Old | Ground water potential | Deposition at lower reaches | Less influenced | Homogenous |
| SW8 | 21.883 | 0.4286 | Culminating stage | Uniform water discharge | Less eroded surface | Influenced | Intrusions and exposed to denudation |
| SW9 | 22.202 | 0.2535 | Old | Intensified run-off | Prone to erosion | Less influenced | Homogenous |
| SW10 | 32.582 | 0.2999 | Old | Uniform water discharge | Less eroded surface | Partially influenced | Exposed to denudation |
| SW11 | 23.808 | 0.3329 | Mature | Uniform water discharge | Less eroded surface | Partially influenced | Intrusions and exposed to denudation |
| SW12 | 71.993 | 0.3173 | Mature | Uniform water discharge | Less eroded surface | Partially influenced | Intrusions and exposed to denudation |
| SW13 | 64.453 | 0.3796 | Culminating stage | Uniform water discharge | Less eroded surface | Influenced | Intrusions and exposed to denudation |
| SW14 | 55.065 | 0.2484 | Old | Ground water potential | Deposition at lower reaches | Less influenced | Homogenous |
| SW15 | 47.799 | 0.2092 | Very old | Ground water potential | Deposition at lower reaches | Less influenced | Homogenous |
| Meenachil river basin | 831.661 | 0.0834 | Monadnock phase | Ground water potential at lower reaches | Prone to erosion, maintained a quasi-equilibrium stage | Less influenced | Homogenous |

*GSD – Geologic Stage of Development

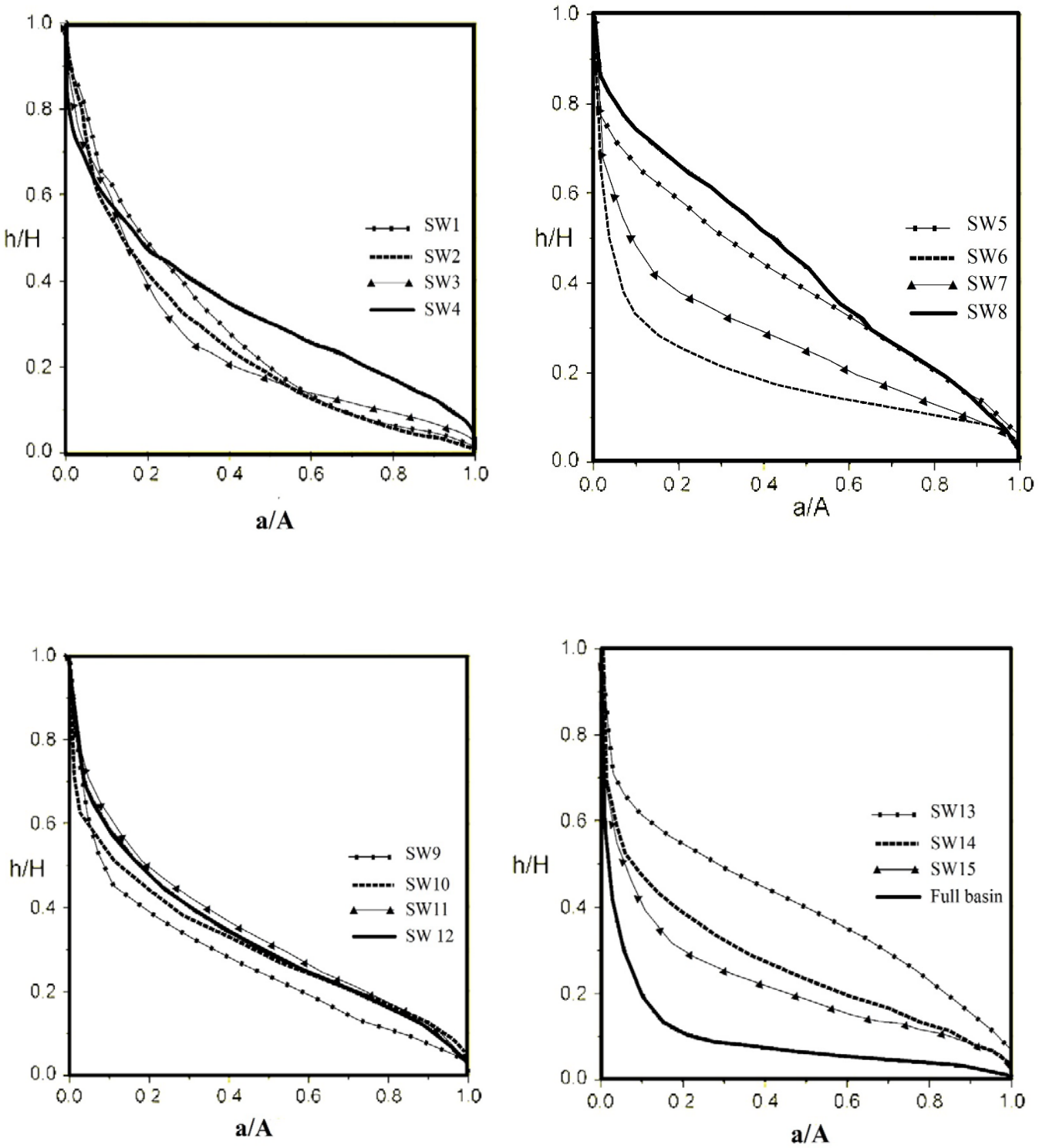


Figure 4. Hypsometric curves of Meenachil River Basin and its 15 sub-watersheds

Among the 15 sub-watersheds, the SW4, SW5, SW8, SW11, SW12 and SW13 is having the hypsometric integral greater than 0.3, indicates the mature stage. Sub-watersheds in mature stage have more susceptibility to erosion when compared to old stage, since these sub watersheds are still in in-equilibrium. The hypsometric integral values of 0.4286 (highest among the tributaries) and 0.0834 (The Meenachil whole basin) of watersheds (Table 1) indicated that 43% and 8% of the original rock masses still exist in these watersheds respectively. It is understood from the analysis that the geology of the watersheds is attaining old stages at higher reaches, while certain watersheds of the lower reaches have been attaining mature stages.

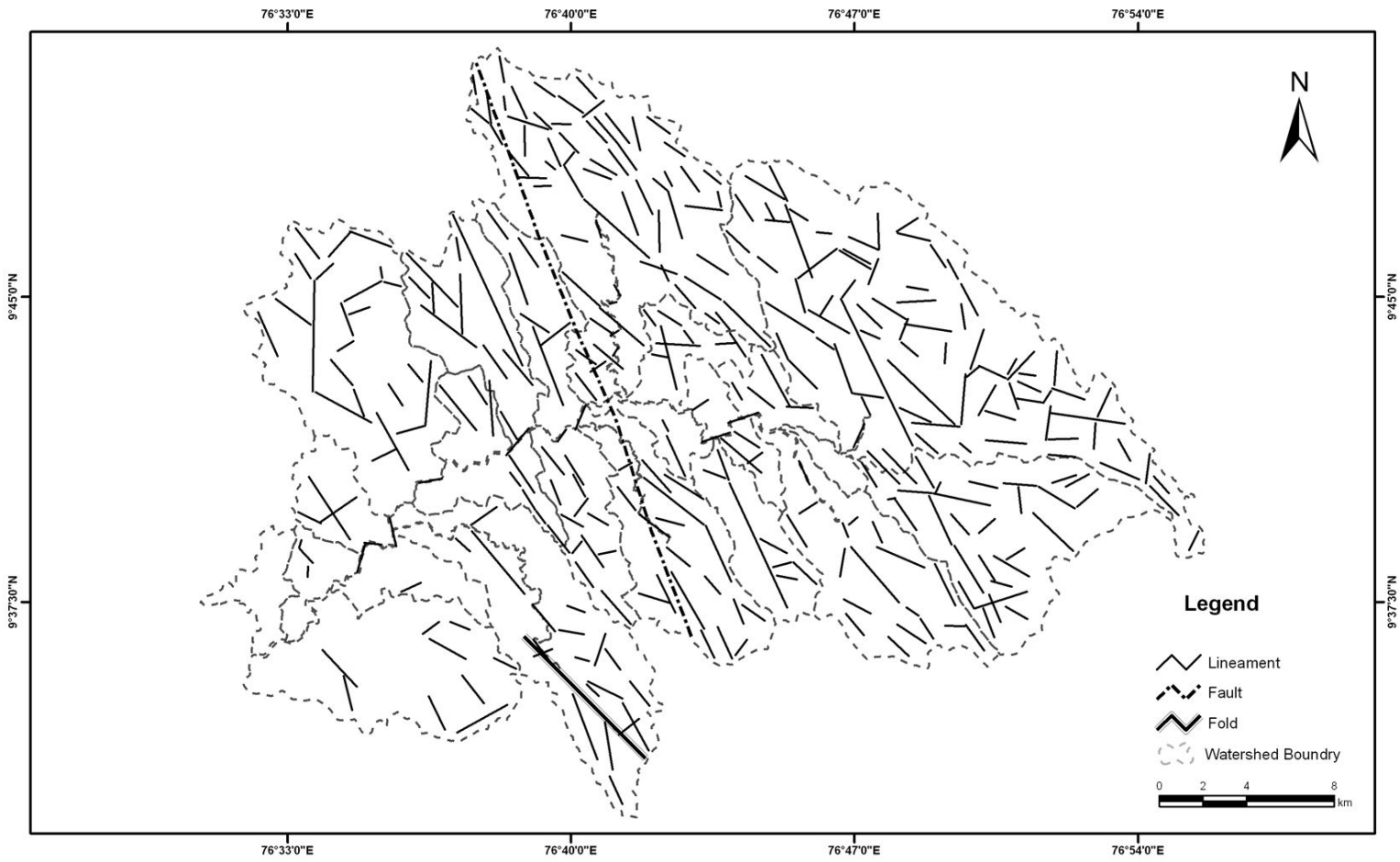


Figure 5. Structural Map of Meenachil River Basin

These watersheds, especially SW4, SW5, SW8, SW11, SW13 (southern side) and SW 12 (northern side) have slow rate of erosion unless there are very high intense storms leading to high runoff peaks as explained by Ritter et al., (2002). The abnormality in the distribution of hypsometric integral values has been evaluated further, since the general principle is that as the river progresses towards the mouth, processes along its longitudinal profile have a change from young to mature to old as suggested by Thornbury (1969) and refined by Rosgen (1994). The analysis suggested that the high hypsometric integral values of the watersheds lying at the lower reaches of the Meenachil River basin are attributed to structural disturbances, especially the neo-tectonic influence in the basin geometry. Hence an evaluation of the structural components of the study has been prepared and the result of which is presented as figure 5. The observations of Ajaykumar et al., (2013) regarding the influence of structural components at the lower reaches of Meenachil river is further clarified with the high hypsometric integral values of SW4, SW5, SW8, SW11, SW12 and SW13 due to the epitomization by a plunging antiformal anticline.

Differences of the hypsometric surfaces are also quantified using the statistical metrics introduced by Harlin (1978): hypsometric integral (I), skewness (SK) and kurtosis (K); and density skewness (DSK) and kurtosis (DK), as shown in Table 2. The configuration of the upland region and the dissected lowlands lends itself to imposing hypsometric changes to the basin that mimic the effects of long-term landscape evolution, as performed in numerical experiments expressed by Willgoose (1994) and Moglen & Bras (1995). The Meenachil basin has attained a quasi-steady state on the drainage-basin scale despite Quaternary climatic fluctuations, as the actively uplifting and eroding landscapes have been adjusted to the mean climatic condition. It is well evident from the hypsometric integral values and the pattern of the hypsometric curve of the SW6. The basin has developed a very old geographical expression with good ground water potential. The pattern of the hypsometric curves of SW6, SW7, SW14 and SW15 suggested that the formation of alluvial deposits made the watershed favourable for groundwater re-charge. The results have ratified those observations made by Whipple (2001) and Singh (2009). The major observations on each watershed based on hypsometric integrals have been tabulated and presented in Table 3.

## 4. CONCLUSION

The evolution of the drainage basins of Western Ghats has an association with Western Ghats orogeny. Since the river basin has age old evolutionary history to unveil, the stages of youth, maturity, and old age in regions of homogeneous rock give a distinctive series of hypsometric forms, while mature and old stages give identical curves unless monadnock masses are present. Hence, the proposal to opt the terminology like an in-equilibrium stage, an equilibrium stage, and a monadnock phase in place of young, mature and old stages respectively is also found relevant here. The hypsometric analysis showed that the drainage basin height, slope steepness, stream channel gradient, and drainage density are having a good negative correlation with mean integrals. Among the 15 sub-watersheds, the SW4, SW5, SW8, SW11, SW12 and SW13 are having the hypsometric integral greater than 0.3, indicates the in-equilibrium stage. Sub-watersheds in in-equilibrium stage have more susceptibility to erosion when compared to equilibrium stage. The analysis also revealed that the lithologic and structural differences between areas or recent minor uplifts may account for certain curve differences as seen in the case of SW4, SW5, SW8, SW11, SW12 and SW13 and the regions of strong horizontal structural benching give a modified series of hypsometric curves. The pattern of the hypsometric curves of SW6, SW7, SW14 and SW15 suggested that the formation of alluvial deposits made the watershed favourable for groundwater re-charge. Hence, the practical application of hypsometric analysis is foreseen in hydrology, soil erosion and sedimentation studies, and military science.

**Acknowledgement**

Dr. B. Ajaykumar expresses the words of gratitude to the Director of Mining and Geology, Govt. of Kerala for his constant encouragement. Dr. Girish Gopinath extends his sincere thanks to the Executive Director, CWRDM for providing the centralized Remote Sensing facility for the analysis.

**REFERENCES**

**Ajaykumar B., Girish Gopinath, & Shylesh Chandran, M.S**., 2013 *River sinuosity in a humid tropical river basin, south west coast of India.* Arabian Journal of Geosciences (Springer). DOI 10.1007/s12517-013-0864-y

**Anderson R.S. & Anderson SP.,** 2010. *Geomorphology: The mechanics and chemistry of landscapes,* Cambridge University Press, New Delhi

**Ascione A., Cinque A., Miccadei E., Villani F. & Berti C.,** 2008. *The Plio-Quaternary uplift of the Apennine chain: new data from the analysis of topography and river valleys in Central Italy.* Geomorphology 102 (1): 105–118.

**Azor A., Keller E.A. & Yeats R.S.,** 2002. *Geomorphic indicators of active fold growth: South Mountain – Oak ridge anticline, Ventura basin, southern California*. The Geological Society of America Bulletin, 114 (6): 745 – 753

**Barbero L., Jabaloy A., Gómez-Ortiz D., Pérez-Peña J.V., Rodríguez-Peces M.J., Tejero R., Estupiñán J., Azdimousa A., Vázquez M. & Asebriy L**., 2010. *Evidence for surface uplift of the Atlas Mountains and the surrounding peripheral plateau: combining apatite fission-track results and geomorphic indicators in the western Moroccan Meseta (coastal Variscan Paleozoic basement).* Tectonophysics 502: 90–104.

**Bertoldi G., Rigon R. & Over T.M.**, 2006. *Impact of watershed geomorphic characteristics on the energy and water budgets*, Journal of Hydrometeorology, 7: 389– 403.

**Bishop M.P., Shroder J.F., Bonk R. & Olsenholler J**., 2002. *Geomorphic change in high mountains: a western Himalayan perspective.* Global and Planetary Change 32: 311–329.

**Brocklehurst S.H. & Whipple K.X**., 2004. *Hypsometry of glaciated landscapes.* Earth Surface Processes and landforms, 29: 907 – 926

**Chen Y., Sung Q. & Cheng K**., 2003. *Along-strike variations of morphotectonic features in the Western Foothills of Taiwan: tectonic implications based on stream-gradient and hypsometric analysis.* Geomorphology 56 (1-2): 109–137

**Cheng K.Y., Hung J.H., Chang H.C., Tsai H. & Sung Q.C.,** 2012. *Scale independence of basin hypsometry and steady state topography.* Geomorphology 171-172: 1-11

**D' Allesandro L., Monte D.M., Fredi P., Palmieri L.E. & Peppolponi S**., 1999. *Hypsometric analysis in the study of Italian drainage basin morphoevolution*, Transactions Japanese Geomorphological Union, 20(3): 187-202.

**Di Benedetto F., Vivoni E.R., & Grimaldi S.,** 2006. *Use of Hypsometric Analysis for a Classification of Basin Hydrological Response: Surface and Groundwater Partitioning.* American Geophysical Union, Fall Meeting 2006, abstract #H31E-1471

**Duffy C.J.,** 1996. *A two-state integral-balance model for soil moisture and groundwater dynamics in complex terrain*, Water Resources Research, 32: 2421-2424

**Eltahir E.A.B. & Yeh P.J.F**., 1999. *On the asymmetric response of aquifer water level to floods and droughts in Illinois*, Water Resources Research, 35: 1199– 1217.

**Hancock G.R. & Willgoose G.R**., 2001. *The interaction between hydrology and geomorphology in a landscape simulator experiment.* Hydrological Processes, 15(1): 115-133.

**Harlin J.M**., 1978. *Statistical moments of the hypsometric curve and its density function*. Mathematical Geology, 10: 59– 72.

**Harlin J.M**., 1980. *The effect of precipitation variability on drainage basin morphometry*. American Journal of Science, 280(8): 812-825.

**Harlin J.M**., 1984. *Watershed morphometry and time to hydrograph peak*, Journal of Hydrology, 67: 141– 154.

**Howard A.D**., 1990. *Role of hypsometry and planform in basin hydrologic response*, Hydrological Processes, 4: 373 – 385.

**Hurtrez J.E, Lucazeau F, Lavé J, & Avouac J.P**., 1999. *Investigation of the relationships between basin morphology, tectonic uplift, and denudation from the study of an active fold belt in the Siwalik Hills, central Nepal*, Journal of Geophysical Research, 104(B6): 12779–12796

**Hutchinson M**., 1989. *A new procedure for gridding elevation and stream line data with automatic removal of spurious pits*, Journal of Hydrology, 106: 211– 232.

**Ijja´sz-Va´squez E.D., Bras R.L. & Moglen G.E**., 1992. *Sensitivity of a basin evolution model to the nature of the runoff production and to initial conditions*, Water Resources Research, 28: 2733 – 2741.

**Ivanov V.Y., Vivoni E.R., Bras R.L. & Entekhabi D**., 2004a. *Catchment hydrologic response with a fully distributed triangulated irregular network model*, Water Resources Research, 40, W11102, doi:10.1029/2004WR003218.

**Ivanov V.Y., Vivoni E.R., Bras R.L. & Entekhabi, D.,** 2004b. *Preserving high-resolution surface and rainfall data in operational-scale basin hydrology: A fully-distributed, physically-based approach*, Journal of Hydrology, 298: 80 – 111.

**Kedareswarudu U., Aravind U.S. & Chattopadhyay M.,** 2013. *Analysis of watershed characteristics and basin management using RS and GIS: A case study from upper provenance of Karamana River, Trivendrum district, Kerala*. International Journal of Remote sensing and Geoscience, 3(1): 36 – 48

**Keller E.A. & Pinter N**., 1996. Active tectonics: Earthquakes, uplift and landscapes. Prentice Hall, New Jersey

**Korup O**., 2006. *Rock-slope failure and the river long profile.* Geology, 34:45–48.

**Korup O., Schmidt J. & McSavenecy M.J.,** 2005. *Regional relief characteristics and denudation pattern of the western Southern Alps, New Zealand*. Geomorphology, 71: 402–423.

**Korup O., Clague J.J., Hermanns R.L., Hewitt K., Strom A.L. & Weidinger J.T.,** 2007. *Giant landslides, topography, and erosion.* Earth and Planetary Science Letters, 261: 578–589.

**Langbein W.B.,** 1947. *Topographic characteristics of drainage basins*, U. S. Geological Survey Water Supply Paper 968-C: 125-157.

**Latron J. & Gallart F.,** 2007. *Seasonal dynamics of runoff-contributing areas in a small Mediterranean research catchment (Vallcebre, eastern Pyrenees)*, Journal of Hydrology, 335: 194 – 206.

**Lifton N.A. & Chase C.G.,** 1992. *Tectonic, climatic and lithologic influences on landscape fractal dimension and hypsometry: Implications for landscape evolution in the San Gabriel Mountains, California*, in R S Snow and L Mayer (Eds.) Fractals in Geomorphology. Geomorphology, 5: 77 – 114

**Liyanagamage S. & Hewa G**., 2012. *Link between flow regime and the catchment hypsometry: Analysis of South Australian Basins.* Journal of Hydrologic Engineering, 17(12): 1287 – 1295

**Luo W**., 1998. *Hypsometric analysis with a geographic information system*, Computers and Geosciences 24: 815 – 821

**Luo W**., 2000. *Quantifying groundwater-sapping landforms with a hypsometric technique*, Journal of Geophysical Research, 105: 1685 – 1694.

**Luo W. & Harlin J.M**., 2003. *A theoretical travel time based on watershed hypsometry*, Journal of the American Water Resources Association, 39: 785–792.

**Mahmood S.A, Yameen M., Sheikh R.A, Rafique H.M. & Almas A.S.,** 2012. *DEM and GIS based hypsometric analysis to investigate neo-tectonic influence on Hazara Kashmir Syntaxis.* Pakistan Journal of Science, 64 (3): 209 - 213

**Marani M., Eltahir E. & Rinaldo A.,** 2001. *Geomorphic controls on regional base flow*, Water Resources Research, 37: 2619 – 2630.

**Markose V.J. & Jayappa K.S.,** 2011. *Hypsometric analysis of Kali River Basin, Karnataka, India, using geographic information system*, Geocarto International, DOI:10.1080/ 10106049.2011.608438

**Moglen G.E & Bras R.L**., 1995. *The effect of spatial heterogeneities on geomorphic expression in a model of basin evolution*, Water Resources Research, 31: 2613– 2623.

**Oertel G.F**., 2001. *Hypsographic, hydro-hypsographic and hydrological analysis of coastal bay environments, Great Machipongo Bay, VA*, Journal of Coastal Research, 17: 775-783

**Ohmori H.,** 1993. *Changes in the hypsometric curve through mountain building resulting from concurrent tectonics and denudation*, Geomorphology, 8: 263–277

**Pedrera A., Pérez-Peña J.V., Galindo-Zaldívar J., Azañón J.M. & Azor A.,** 2009. *Testing the sensitivity of geomorphic indices in areas of low-rate active folding (eastern Betic Cordillera, Spain).* Geomorphology 105: 218–231.

**Pike R.J. & Wilson S.E**., 1971. *Elevation-relief ratio, hypsometric integral and geomorphic area-altitude analysis*, Geological Society of America Bulletin, 82: 1079 – 1084

**Ramu & Mahalingam B**., 2012. *Hypsometric properties of drainage basins in Karnataka using Geographical Information System.* New York Science Journal, 5 (12): 156 – 158

**Ritter D.F, Kochel R.C. & Miller J.R.,** 2002. Process Geo.morphology, McGraw Hill, Boston.

**Rodrı´guez-Iturbe I. & Valdes J.B.,** 1979. *The geomorphologic structure of the hydrologic response*, Water Resources Research, 15: 1409 – 1420.

**Rosgen D.L**., 1994. *A classification of natural rivers.* Catena, 22: 169 – 199

**Schumm S.A**., 1956. *Evolution of drainage systems and slopes in badlands at Perth Amboy, New Jersey*, Geological Society of America Bulletin, 67: 597–646.

**Shahzad F. & Gloaguen R.,** 2011. *TecDEM: A MATLAB based toolbox for tectonic geomorphology, part 2: surface dynamics and basin analysis.* Computers and Geosciences, 37: 261 - 271

**Singh O**., 2009. *Hypsometry and erosion proneness: a case study in the lesser Himalayan watersheds.* Journal of soil and water conservation, 8 (2): 53 – 59

**Sinha R.S**., 2002. *Hypsometry and Landform Evolution: A case Study in the Banas Drainage Basin, Rajasthan, with Implications for Aravalli Uplift*, Journal of Geological Society of India, 60: 7-26.

**Sivakumar V, Biju C. & Deshmukh B.,** 2011. *Hypsometric analysis of Varattaru river basin of Harur taluk, Dharmapuri district, Tamil Nadu, India using geomatics technology.* International journal of Geomatics and Geosciences, 2(1): 241 – 247

**Strahler A.N**., 1952. *Hypsometric (area-altitude) analysis of erosional topography*, Geological Society of America Bulletin, 63(11): 1117-1142

**Strahler A.N**., 1964. *Quantitative geomorphology of drainage basins and channels networks.* In Chow VT, (Ed) Handbook of Applied Hydrology. McGraw Hill Book Company, New York.

**Tarboton D.G., Bras R.L. & Rodrı´guez-Iturbe I.,** 1992. *A physical basis for drainage density*, Geomorphology, 5: 59– 76.

**Thornbury W.D.,** 1969. Principles of Geomorphology (2nd Edition), Wiley, New York

**Tucker G.E. & Bras R.L.,** 1998. *Hillslope processes, drainage density, and landscape morphology*, Water Resources Research, 34: 2751 – 2764.

**Vivoni E.R., Entekhabi D., Bras R.L. & Ivanov V.Y.,** 2007. *Controls on runoff generation and scale-dependence in a distributed hydrologic model*, Hydrology and Earth System Science, 11: 1683– 1701.

**Vivoni E.R., Di Benedetto F., Grimaldi S. & Eltahir E.A.B.,** 2008. *Hypsometric control on surface and subsurface runoff*, Water Resources Research, 44 (12), W12502, doi:10.1029/ 2008WR006931.

**Vivoni E.R., Ivanov V.Y., Bras R.L. & Entekhabi D.,** 2004. *Generation of triangulated irregular networks based on hydrological similarity*, Journal of Hydrologic Engineering, 9: 288– 302.

**Vivoni E.R., Ivanov V.Y., Bras R.L. & Entekhabi D.,** 2005. *On the effects of triangulated terrain resolution on distributed hydrologic model response*, Hydrological Processes, 19: 2101–2122

**Walcott R.C. & Summerfield M.A.,** 2008. *Scale dependence of hypsometric integrals: An analysis of southeast African basins.* Geomorphology, 96(1-2): 175 -186

**Weissel J.K., Pratson L.F. & Malinverno A.,** 1994. *The length-scaling properties of topography*, Journal of Geophysical Research, 99: 13997–14012.

Whipple KX (2001) Fluvial landscape response time: How plausible is steady state denudation. American Journal of Science, 301: 313 – 325

**Willgoose G.,** 1994. *A statistic for testing the elevation characteristics of landscape simulation models*, Journal of Geophysical Research, 99: 13987 – 13996.

**Willgoose G. & Hancock G.,** 1998. *Revisiting the hypsometric curve as an indicator of form and process in transport-limited catchment*, Earth Surface Processes and Landforms, 23: 611 – 623.

**Zecharias Y.B. & Brutsaert W**., 1988. *The influence of basin morphology on groundwater outflow*, Water Resources Research, 24: 1645 – 1650.

Received at: 17. 10. 2017
Revised at: 12. 03. 2018
Accepted for publication at: 15. 03. 2018
Published online at: 19. 03. 2018